FISEVIER

Contents lists available at ScienceDirect

Journal of Non-Newtonian Fluid Mechanics

journal homepage: www.elsevier.com/locate/jnnfm



Full length article



Approach to a similarity solution of the lubrication flow of an Oldroyd-B fluid through a hyperbolic pipe

John Hinch

Department of Applied Mathematics and Theoretical Physics, University of Cambridge, Cambridge, CB3 0WA, United Kingdom

ARTICLE INFO

Keywords: Contraction Lubrication flow Oldroyd-B Pressure drop Stress jump Summing series

ABSTRACT

Sialmas & Housiadas (2025), found a similarity solution of the Oldroyd-B equations for viscoelastic flow through a slowly varying axisymmetric contraction with a hyperbolic shape. We study whether inlet stresses decay onto this similarity solution before the end of the pipe, finding they do so only when a strain-rate based Deborah number is sufficiently small, $De_s \leq 1$.

1. Introduction

Sialmas & Housiadas [1] recently published an intriguing "exact solution" of the Oldroyd-B equations for flow through a slowly varying hyperbolic contraction, their Eq. (45). That solution does not match the stresses at the inlet from a preceding straight cylindrical pipe, their boundary conditions (35). Sialmas & Housiadas give no immediate warning that they have failed to satisfy their inlet boundary condition

There is a complication in the boundary conditions on the polymer stress when the geometry has a jump in the slope, as there is in the chosen shape, their (17), with R'(0-)=0 and $R'(0+)=-\frac{1}{2}\beta$ (with radius varying R(z) replacing their height H(z)). This jump in slope at the entrance to the contraction leads to a jump in the cross-flow component of velocity v, at least as appears on the long length scale of the slowly varying contraction. (There is a rapid change over an axial distance equal to one diameter of the pipe.) This jump in velocity leads to a delta-function in the vorticity. This spike in vorticity leads to a rapid rotation of the polymer stresses (with no time to relax), so that

$$\sigma_{zz}(0+) = \sigma_{zz}(0-),\tag{1}$$

$$\sigma_{yz}(0+) = \sigma_{yz}(0-) - \frac{1}{2}\beta Y \sigma_{zz}(0-), \tag{2}$$

$$\sigma_{yy}(0+) = \sigma_{yy}(0-) - \beta Y \sigma_{yz}(0-) + \frac{1}{4} (\beta Y)^2 \sigma_{zz}, \tag{3}$$

where Y = y/R(z). Sialmas & Housiadas [1] seem unaware of this complication. This complication does not arise if the geometry is smooth without a jump in slope, and does not arise in the hyperbolic contraction if using the orthogonal curvilinear coordinates of Hinch, Boyko & Stone (2024) [2].

So the new "exact solution" of Oldroyd-B equations satisfies neither the declared nor the correct inlet boundary conditions on the stress.

It is one of an infinite number of possible solutions of the differential equations. It is however a privileged solution. It is a similarity solution, just as in the Blasius (1908) boundary layer and the Schlicting (1932) momentum jet.

Sialmas & Housiadas assume in the first sentence of their §4.2, together with Eq. (20), a certain dependence of the velocity, shearrates and stresses along the streamlines, with an unknown self-similar form across the streamlines. This similarity form is substituted into the governing equations to yield an ordinary differential equation for the variation across the streamlines.

In common with all other similarity solutions, there are three tests to whether the solution is applicable, in other words is realisable. First, a solution of the ordinary differential equation has to exist. Second, it must be stable. Finally, other solutions of the original partial differential equations must decay onto it. The "exact solution" of Sialmas & Housiadas obviously passes the first test, because they have exhibited a closed form analytic solution. In this problem, the second test is answered by the third test. This paper addresses the third test of whether other solutions decay onto the similarity solution; the key question of interest. It is found that the relaxation time must be shorter than the residence time, more precisely if $De_e \lesssim 1$. Hereafter the "exact solution" will be referred to as the *similarity solution*, and the solution which satisfies the inlet conditions will be called the *full solution*.

The governing equations are set out in Section 2 following the approach and notation of [2], adapted to the axisymmetric pipe geometry. It will be assumed that the velocity profile remains the Newtonian parabolic form. That permits a rescaling of the deformation of the microstructure that incorporates the stretching of material line elements. The geometry will be taken to be a hyperbolic contraction. The

E-mail address: ejh1@cam.ac.uk.

pressure drop will be found for just the contraction section, ignoring further viscoelastic changes to the total pressure drop occurring in the

Section 3 gives a first look at how the inlet stresses evolve and whether or not they tend to the similarity solution. Some consequences on the pressure drop are presented.

Section 4 considers an expansion in small Deborah number. The mathematical structure of a naive expansion offers no opportunity to satisfy a boundary condition on the inlet elastic stresses. Terms beyond the leading order fail to satisfy the inlet condition if there is a jump in the shape of the geometry, as there is for a hyperbolic contraction abruptly attached to a straight entry pipe. For the hyperbolic contraction, the terms in the naive expansion take a simple form that can be summed. The sum is exactly the similarity solution of [1]. That similarity solution fails to satisfy the inlet condition, increasingly so as the Deborah number increases. The very good agreement between the similarity solution and the low-De expansion in [1] is due to the sum of the expansion being exactly the similarity solution. The very good agreement offers no support that either are valid.

Section 5 derives the full solution as an additional part that must added to the similarity solution in order to satisfy the inlet condition on the elastic stress. The low-De expansion of this additional part finds the leading term in the pressure drop is $O(De^2)$ with a relatively small coefficient. Higher-order terms also have small coefficients compared with the expansion of the similarity solution. This explains how for the pressure drop the similarity solution agrees so well with the correct full solution at low De. Examining the integral of the pressure gradient through the contraction finds a dramatic change at $De_e = O(1)$. For smaller De_e , the pressure drop from the additional part of the solution occurs near the inlet. At $De_e = O(1)$ the main pressure drop switches to the outlet, in a manner reminiscent of the behaviour in exponential asymptotics, in say the Airy function. This switch explains how the remarkably good agreement at low De is lost at higher De.

2. Governing equations

2.1. Lubrication approximation

In this section, we set out the governing equations following the approach and notation in [2], adapted to the axisymmetric pipe geometry. Stress in the Oldroyd-B fluid is considered to be a simple combination of a viscous stress $2\mu_0$ e and an elastic stress GA, the elastic microstructure A being stretched and sheared according to Oldroyd's upper-convected derivative and relaxing to the isotropic state on a time scale τ . The flow takes place through a slowly varying axisymmetric contraction, with a radius r = R(z) in $0 \le z \le \ell$, with slowly-varying parameter

$$\epsilon = R(0)/\ell \ll 1$$
.

In the standard lubrication scalings, we non-dimensionalise the axial distance z by ℓ , and the radial distance r and local radius R(z) by R(0). With volume flux πQ , we non-dimensionalise the axial velocity w by $Q/R^2(0)$ and the radial velocity v by $Q/R(0)\ell$, time t by the residence time $\ell R^2(0)/Q$, and pressure p by $\mu_0 Q \ell / R^4(0)$. There are three nondimensional parameters, a reduced Reynolds number $Re = \rho Q/\mu_0 \ell$, a polymer concentration $c = G\tau/\mu_0$, and an entrance Deborah number $De = Q\tau/R^2(0)\ell$. We assume that inertia can be ignored, $Re \ll 1$, that the polymer concentration is small $c \ll 1$ so that the velocity field remains that of a Newtonian fluid, and that De = O(1). To promote the non-Newtonian tension in the streamlines, the different components of the microstructure are scaled differently with the slowly-varying parameter ϵ : A_{rr} and $A_{\theta\theta}$ by ϵ^0 , A_{zr} by ϵ^{-1} , and A_{zz} by ϵ^{-2} .

We assume that the flow has no swirl, i.e. $\mathbf{u} = (v(r, z), 0, w(r, z))$. Conservation of mass becomes

$$\nabla \cdot \mathbf{u} = \frac{1}{r} \frac{\partial (rv)}{\partial r} + \frac{\partial w}{\partial z} = 0.$$

The axial component of the momentum equation becomes

$$0 = -\frac{dp}{dz} + \frac{1}{r} \frac{\partial}{\partial r} \left(r \frac{\partial w}{\partial r} \right) + \frac{c}{De} \left(\frac{1}{r} \frac{\partial (rA_{rz})}{\partial r} + \frac{\partial A_{zz}}{\partial z} \right).$$

Oldroyd-B in the axisymmetric cylindrical geometry becomes

$$\begin{split} \mathbf{u} \cdot \boldsymbol{\nabla} A_{rr} - 2e_1 A_{rr} & -2\gamma_1 A_{rz} = -\frac{1}{De} \left(A_{rr} - 1 \right), \\ \mathbf{u} \cdot \boldsymbol{\nabla} A_{rz} - e_2 A_{rz} & -\gamma_2 A_{rr} & -\gamma_1 A_{zz} = -\frac{1}{De} A_{rz}, \end{split}$$

$$\mathbf{u} \cdot \nabla A_{rz} - e_2 A_{rz} - \gamma_2 A_{rr} - \gamma_1 A_{zz} = -\frac{1}{De} A_{rz}$$

$$\mathbf{u} \cdot \nabla A_{zz} - 2e_3 A_{zz} - 2\gamma_2 A_{rz} = -\frac{1}{De} A_{zz},$$

$$\mathbf{u} \cdot \nabla A_{\theta\theta} - 2e_4 A_{\theta\theta} = -\frac{1}{De} (A_{\theta\theta} - 1),$$

$$\mathbf{u} \cdot \mathbf{\nabla} = v \frac{\partial}{\partial r} + w \frac{\partial}{\partial z},$$

$$\gamma_1 = \frac{\partial v}{\partial z}, \quad \gamma_2 = \frac{\partial w}{\partial r},$$

and strain-rates

$$e_1 = \frac{\partial v}{\partial r}, \quad e_2 = \frac{\partial w}{\partial z} + \frac{\partial v}{\partial r}, \quad e_3 = \frac{\partial w}{\partial z}, \quad e_4 = \frac{v}{r}.$$

Results will be obtained for a contraction with a hyperbolic shape

$$R(z) = \frac{1}{(1 + \beta z)^{1/2}}. (4)$$

This has an overall area-contraction of $1+\beta$, so the velocity will increase by this factor, the shear rates by $(1 + \beta)^{3/2}$ and the normal stresses by $(1+\beta)^3$. The experiments of James & Roos [3] have an area-contraction of 20, while the numerical study of Sialmas & Housiadas [1] has an area-contraction of 16. Note that these large contraction ratios have a very large increase in the normal stresses within the contraction, by 8000 and by 4000 respectively. These large increases can make numerical calculations challenging. Despite this, a value of $\beta = 15$ will be used in most of the examples in this paper.

At the start of this subsection, the entrance Deborah number was defined as the average velocity across the entrance, multiplied by the relaxation time, and divided by the length of the contraction, De = $(Q/R_0^2)\tau/\ell$. There are several other possible definitions, each with some merit. A Deborah number based on the faster flow at the exit is De_{ℓ} = $De(1 + \beta)$. A Deborah number based on the strain-rate averaged over the entrance is $De_e = De\beta$. This Deborah number will be discussed further in Section 4. Finally the traditional definition as the ratio of the relaxation time to a residence time (travelling at the velocity averaged across each section) is $De_t = De\beta / \ln(1 + \beta)$. In this paper, the entrance Deborah number De and the strain-rate Deborah number De_e will play key roles. James & Roos [3] use a Deborah number based on the strainrate, but use the maximum velocity in the cross-section instead of the average velocity here, so $De_{JR} = 2De_e$. James & Roos also drop a factor of π in their Eq. (4), although include the π in the calculation of $3.4 \, s^{-1}$. The maximum Deborah number in the experiments of James & Roos was their $De_{JR} = 4.4$. Sialmas & Housiadas [1] use a Deborah number based on the strain-rate, but use half the average velocity, so their $De_m = \frac{1}{2}De_e$.

2.2. Curvilinear coordinates

It is convenient to map the geometry of the contraction on to a unit

$$0 \le z \le 1, \quad 0 \le \rho = \frac{r}{R(z)} \le 1.$$

The coordinate lines z = const. and $\rho = \text{const.}$ are not orthogonal in the zr-plane, due to the slope R'(z). Transforming partial differential equations is much easier with orthogonal curvilinear coordinates. Because the slope of the boundary is $O(\epsilon)$ small in the slowly-varying geometry, only a small displacement in the z direction is necessary to create an orthogonal system

$$z(\zeta,\rho) = \zeta + \epsilon^2 \frac{1}{4} (R^2(\zeta))'(1-\rho^2) + O(\epsilon^4), \quad r(\zeta,\rho) = R(\zeta)\rho.$$

In the previous subsection, we used w for the downstream z-component of velocity and v for the cross-stream r-component. Henceforth we change to use w for the velocity in the downstream ζ -direction, and v for the flow in the cross-stream ρ -direction. There is a negligible $O(\epsilon^2)$ difference between the flow w in the ζ - and z-directions. However the flow in the r-direction is greater by wR' than the flow v in the ρ -direction, because the small slope R' is multiplied by a large downstream velocity w. In a similar way, we shall use A_{11} , A_{12} and A_{22} for the components of the microstructure in the $\zeta \zeta$ -, $\zeta \rho$ - and $\rho \rho$ -directions. As with the velocity, there is a negligible $O(\epsilon^2)$ difference between A_{11} and A_{zz} , and O(1) differences between the other curvilinear and Cartesian components, see Appendix A of Boyko, Hinch & Stone [4].

With little difference between z and ζ , henceforth derivatives with respect to ζ will be written as with respect to z.

In these curvilinear coordinates, the governing equations become for mass

$$\nabla \cdot \mathbf{u} = \frac{1}{R\rho} \frac{\partial}{\partial \rho} (\rho v) + \frac{1}{R^2} \frac{\partial}{\partial z} (R^2 w) = 0,$$

and axial momentum,

$$0 = -\frac{dp}{dz} + \frac{1}{R^2\rho}\frac{\partial}{\partial\rho}\left(\rho\frac{\partial w}{\partial\rho}\right) + \frac{c}{De}\left(\frac{1}{R\rho}\frac{\partial}{\partial\rho}(\rho A_{12}) + \frac{1}{R^2}\frac{\partial}{\partial z}(R^2A_{11})\right).$$

The Oldroyd-B equations are little changed,

$$\mathbf{u} \cdot \nabla A_{22} - 2e_1 A_{22}$$
 $-2\gamma_1 A_{12} = -\frac{1}{De} (A_{22} - 1),$

$$\mathbf{u}\cdot \nabla A_{12} - e_2 A_{12} \ - \gamma_2 A_{22} \ - \gamma_1 A_{11} \ = - \ \frac{1}{De} A_{12},$$

$$\mathbf{u} \cdot \nabla A_{11} - 2e_3 A_{11} - 2\gamma_2 A_{12} = -\frac{1}{De} A_{11},$$

$$\mathbf{u} \cdot \nabla A_{\theta\theta} - 2e_4 A_{\theta\theta} = -\frac{1}{De} (A_{\theta\theta} - 1),$$

where now

$$\mathbf{u} \cdot \mathbf{\nabla} = \frac{v}{R} \frac{\partial}{\partial \rho} + w \frac{\partial}{\partial z},$$

and with shear-rates

$$\gamma_1 = R \frac{\partial}{\partial z} \left(\frac{v}{R} \right), \quad \gamma_2 = \frac{1}{R} \frac{\partial w}{\partial \rho},$$

and strain-rates

$$e_1 = \frac{1}{R} \frac{\partial v}{\partial \rho} + \frac{R'}{R} w, \quad e_2 = \frac{1}{R} \frac{\partial (Rw)}{\partial z} + \frac{\partial v}{\partial \rho}, \quad e_3 = \frac{\partial w}{\partial z}, \quad e_4 = \frac{v}{R\rho} + \frac{R'}{R} w.$$

Note again $e_1 + e_3 + e_4 = 0$ by mass conservation.

The computationally expensive Poisson problem for the pressure is avoided in lubrication theory where the pressure gradient is locally determined at each downstream section by the constraint that the volume flux is the given constant. Integrating the volume flux by parts a couple of times,

$$1 = R^2 \int_0^1 w \, 2\rho d\rho = -R^2 \int_0^1 \frac{1}{2} (1 - \rho^2) \frac{1}{\rho} \frac{\partial}{\partial \rho} \left(\rho \frac{\partial w}{\partial \rho} \right) \rho d\rho.$$

Substituting from the axial momentum equation, we have an expression for the local pressure gradient

$$\frac{dp}{dz} = -\frac{8}{R^4} + \frac{c}{De} \int_0^1 \left[2(1 - \rho^2) \frac{1}{R^2} \frac{\partial}{\partial z} \left(R^2 A_{11} \right) + \frac{1}{R} 4 \rho A_{12} \right] 2\rho d\rho.$$

This expression can equally be derived from a consideration of the mechanical work done.

2.3. The b-representation

At this stage we assume that the velocity has the Newtonian parabolic form. This is true in the dilute limit $c\ll 1$, and was found

in [2] to be a good approximation in a planar geometry at c=1, a contraction ratio of 2 and De=0.5, where the velocity deviated by less than 6% while the pressure drop was reduced by 40%. With the profile fixed, the magnitude of the velocity must increase inversely with the cross-sectional area, $w \propto R^{-2}(z)$. The streamlines all follow the shape of the hyperbolic boundary. Hence the fluid on each streamline sees a uniaxial straining motion. Further, in our curvilinear coordinates the cross component of the velocity vanishes, v=0. With the volume flux normalised to be π , we therefore have

$$v = 0$$
, $w = \frac{1}{R^2(z)}F(\rho)$, with $F(\rho) = 2(1 - \rho^2)$.

The various shear-rates and strain-rates become

$$\gamma_1 = 0$$
, $\gamma_2 = \frac{1}{R^3} f$, $e_1 = \frac{R'}{R^3} F$, $e_2 = -e_1$, $e_3 = -2e_1$, and $e_4 = e_1$,
where $f(a) = F' = -4a$

It is assumed that prior to the contraction there is a long straight pipe of uniform diameter. The elastic deformation at the entrance to the contraction at z=0 is then

$$A_{22} = A_{\theta\theta} = 1$$
, $A_{12} = Def$, and $A_{11} = 2De^2f^2$.

There is no jump in the elastic stress at the entrance as seen in the curvilinear coordinates, because there is no jump in the component of velocity v.

The b-representation introduced by [2] in §6.3 builds in the Oldroyd upper-convective derivative; that streamwise material line elements stretch proportional to w(z), so proportional to $R(z)^{-2}$, while material line elements in the cross-stream directions are squashed proportional to R(z). This is an adaptation of Renardy's transformation [5] for steady planar flow of an Oldroyd-B fluid. Thus

$$A_{22} = R^2 b_{22}, \quad A_{12} = \frac{Def}{R} b_{12}, \quad A_{11} = \frac{2De^2 f^2}{R^4} b_{11}, \quad A_{\theta\theta} = A_{22}.$$
 (5)

The Oldroyd equations then take a particularly simple form

$$b_{22}' = -\frac{R^2}{DeF} \left(b_{22} - R^{-2} \right), \tag{6a}$$

$$b'_{12} = -\frac{R^2}{DeF}(b_{12} - b_{22}),\tag{6b}$$

$$b'_{11} = -\frac{R^2}{DeF}(b_{11} - b_{12}),\tag{6c}$$

where the prime denotes partial differentiation with respect to z. The inlet conditions are

$$b_{22} = b_{12} = b_{11} = 1$$
, at $z = 0$ for all ρ . (7)

The expression for the pressure gradient becomes

$$\frac{dp}{dz} = -\frac{8}{R^4} + c \int_0^1 \left(2DeFf^2 \frac{1}{R^2} \frac{\partial}{\partial z} \left(\frac{b_{11}}{R^2}\right) - f^2 \frac{b_{12}}{R^2}\right) 2\rho d\rho.$$

The first term on the right hand side is the pressure gradient from the Newtonian viscous solvent. The integral second term is from the elastic stresses. The net pressure drop for flow of the Newtonian solvent through the contraction is

$$\Delta p_0 = \int_0^1 \frac{8}{R^4(z)} \, dz. \tag{8}$$

We define the elastic contribution to the pressure drop to be

$$\Delta p_e = \int_0^1 \int_0^1 \left(-2 DeF f^2 \frac{1}{R^2} \frac{\partial}{\partial z} \left(\frac{b_{11}}{R^2} \right) + f^2 \frac{b_{12}}{R^2} \right) 2 \rho d\rho \, dz, \tag{9}$$

so that the total pressure drop is

$$\Delta p = \Delta p_0 + c \Delta p_e.$$

In the limit of vanishing De, Oldroyd-B behaves as Newtonian viscous fluid, so

$$\Delta p_e = \Delta p_0$$
 at $De = 0$.

For the hyperbolic contraction $\Delta p_0 = 8(1 + \beta + \frac{1}{3}\beta^2)$.

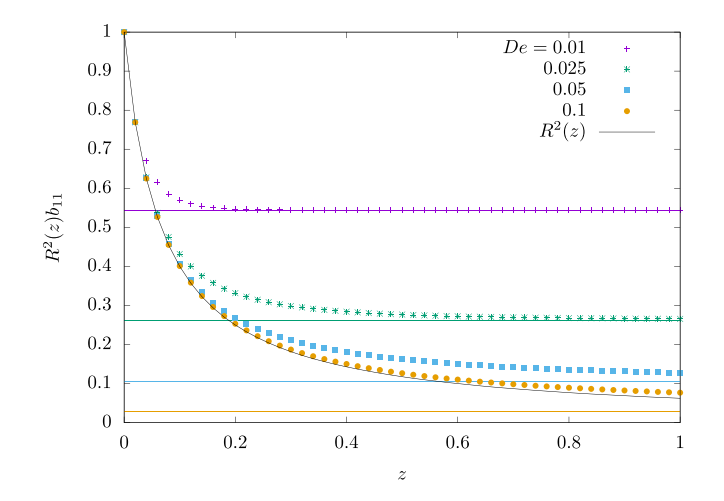


Fig. 1. The evolution down the contraction of the axial stress $R^2b_{11}=A_{11}/(2De^2f^2/R^6)$ at different entrance Deborah numbers De, for $\beta=15$ and for the mid-streamline $\rho=0.5$ so F=1.5. The curves of points are numerical solutions of (6). The horizontal lines are the predictions of the similarity solution (15). The black curve is the high-De behaviour of $b_{11}\sim 1$.

3. First results

To obtain the full solution, the Oldroyd-B equations in the form (6) are integrated numerically along each streamline, $\rho={\rm cont.}$, starting from the inlet conditions (7). Simultaneously the contribution of that streamline to the pressure drop in (9) is evaluated. On the boundary $\rho=1$, the flow vanishes, F=0, so Eq. (6) becomes ill-defined. However, the solution there is that of a steady shear, $b_{11}=b_{12}=b_{22}=R^{-2}$. Finally the contributions from the different streamlines to the pressure drop, (9), are combined. Second-order accurate finite differences are used. At a typical value of the parameters, De=0.2 and $\beta=15$, a test is made with four resolutions to prove that the error decreases quadratically with the resolution, and to ascertain the resolution required for 3-figure accuracy, $\delta x=0.05$. Thereafter spot checks are made at more extreme values of the parameters. The run time was typically a second on a laptop.

We first look in Fig. 1 at how the stresses evolve as they flow through the contraction, starting at the inlet value and possibly tending to the value of the similarity solution. Sialmas & Housiadas [1] in their Fig. 2 show the evolution of the cross-stream component σ_{vv} evaluated on the centreline. That component plays no role in lubrication dynamics. Instead we will look at the dynamically significant component A_{11} describing the tension in the streamlines, and evaluate it on the mid-streamline $\rho = 0.5$. We remove the shear-rate factor by plotting $R^2b_{11} = A_{11}/(2De^2f^2/R^6)$. The similarity solution shown later in (15) has R^2b_{11} constant along the streamline, a constant that depends on the local streamline Deborah number $De\beta F(r)$. The inlet condition (7) is $R^2b_{11} = 1$. Numerical solutions for the full solution of R^2b_{11} are plotted by curves of points in Fig. 1 for various entrance Deborah numbers De. The horizontal lines are predictions of the similarity solution (15). We see that the stresses relax from the inlet value towards the similarity solution. Lower De decay faster and less. At De = 0.01 and 0.025, the inlet stresses relax onto the similarity values 0.5440 and 0.2621 by z = 0.2 and 0.6 respectively. For the higher De = 0.05 and 0.1, there is insufficient residence time for the inlet stresses to relax onto the similarity values 0.1042 and 0.0291. The black curve is a prediction for the high De behaviour, that b_{11} remains equal to the inlet value of 1, because at high De there is no time for any relaxation within the contraction. It is clear that the inlet stresses will never decay to the similarity value if at the end of the contraction $R^2 = 1/(1 + \beta)$ exceeds

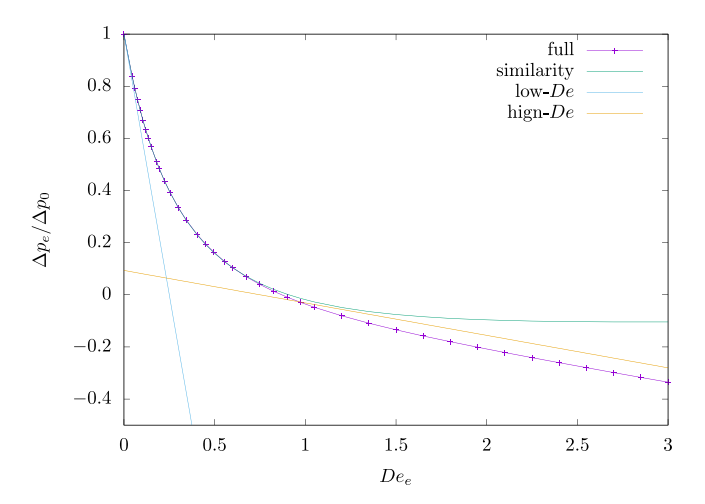


Fig. 2. The elastic contribution to the pressure drop Δp_e , Eq. (9), scaled by the De=0 value Δp_0 , as a function of the strain-rate Deborah number De_e , for an axisymmetric hyperbolic area-contraction ratio of $1+\beta=16$. The curve with points is for the full solution, while the curve without points is for the similarity solution. Also plotted the low-De asymptotic result $1-4De_e$ and the high-De asymptotic result $(-\frac{4}{3}De_e+1)(1+\frac{1}{3}\beta)/(1+\beta+\frac{1}{3}\beta^2)$.

the constant value of the similarity solution $1/(1 + De_e F)^3$, i.e. if

$$De_{\alpha}F > (1+\beta)^{1/3} - 1.$$
 (10)

For $\beta=15$ and F=1.5, this predicts the similarity solution not being achieved if $De_e>1.01$, i.e. De>0.0675, which is a small over estimate of the 0.05 in Fig. 1. The important conclusion is that the similarity solution fails to predict the correct levels of stress once $De_e \gtrsim 1$.

There is something wrong with figure 2 of Sialmas & Housiadas [1] which shows that $\sigma_{yy}(0,z)$ drops further for smaller De and all the different De decay over the same short distance, quite contrary to Fig. 1 here.

Fig. 2 gives numerical results for the elastic contribution to the pressure drop, Eq. (9), as a function of the strain-rate Deborah number De_e , for the full solution and for the similarity solution. Both solutions have the pressure drop decreasing with increasing Deborah number. The two solutions agree remarkably well for $De_e < 1$ and then diverge, and this behaviour must be explained. The full solution decreases linearly at high De while the similarity solution tends to zero. The mechanisms causing this decrease in the full solution were given by Hinch, Boyko & Stone [2]. The primary mechanism, which gives the linear decrease at high De, is that the higher tension in the streamlines at the exit pull the flow through the contraction so requiring less pressure to push the flow. A secondary mechanism is that the elastic shear stresses take time to increase to their new equilibrium values, so providing less friction on the boundary. The mechanisms behind the reduction in the pressure drop for the similarity solution is postponed to the following section, in which details of the similarity solution will be derived.

Additional checks on the numerical results for the full solution are provided by simple low-De and high-De asymptotic predictions. We shall find soon in the next section, Eq. (11), that at low-De

$$\Delta p_e = 8 \int_0^1 \frac{1}{R^4(z)} dz - \frac{32 De}{3} \left(\frac{1}{R^6(1)} - \frac{1}{R^6(0)} \right) + \cdots$$

for a general contraction, and for a hyperbolic contraction $\Delta p_e = \Delta p_0 (1-4De_e+\cdots)$. It is seen in Fig. 2, that this asymptotic prediction agrees with the numerical results in $De_e < 0.05$. At high De, the b-components do not change from their inlet values, $b_{11} \sim 1$ and $b_{12} \sim 1$. Hence for a

general contraction

$$\Delta p_e \sim -\frac{16De}{3} \left(\frac{1}{R^4(1)} - \frac{1}{R^4(0)} \right) + 8 \int_0^1 \frac{1}{R^2(z)} dz,$$

and for hyperbolic contraction $\Delta p_e \sim 8(1+\frac{1}{2}\beta)(-\frac{4}{3}De_e+1)$. This asymptotic prediction agrees with the trend in the numerical results in $De_e \geq 1.5$. There is a 6% difference at $De_e = 3$, which decreases to 2% at $De_e = 15.0$.

4. Naive expansion in small De, and the similarity solution

If we naively regard the problem of finding the low-*De* behaviour as a regular perturbation problem, *which* it is not, one can argue as follows. At low *De*, relaxation dominates, and so to leading order the terms on the right hand side of (6) balance amongst themselves, giving

$$b_{22} \sim R^{-2}$$
, $b_{12} \sim R^{-2}$, $b_{11} \sim R^{-2}$.

This leading order satisfies the inlet boundary conditions. Substituting the leading order into the left hand side of (6) forces the first, O(De), correction

$$b_{22} \sim \frac{1}{R^2} - \frac{DeF}{R^2} \left(\frac{1}{R^2}\right)', \quad b_{12} \sim \frac{1}{R^2} - 2\frac{DeF}{R^2} \left(\frac{1}{R^2}\right)',$$

$$b_{11} \sim \frac{1}{R^2} - 3\frac{DeF}{R^2} \left(\frac{1}{R^2}\right)'.$$
(11)

Clearly one needs R'(0) = 0 if this first correction is to satisfy the inlet stress boundary condition. Continuing to further terms for b_{22}

$$b_{22} = \frac{1}{R^2} - \frac{DeF}{R^2} \left(\frac{1}{R^2}\right)' + \frac{De^2F^2}{R^2} \left(\frac{1}{R^2} \left(\frac{1}{R^2}\right)'\right)'$$
$$- \frac{De^3F^3}{R^2} \left(\frac{1}{R^2} \left(\frac{1}{R^2} \left(\frac{1}{R^2}\right)'\right)'\right)' + \cdots$$
(12)

Clearly one needs R''(0) = 0 for the second correction to satisfy the boundary conditions, and for the third R'''(0) = 0. For the hyperbolic contraction, all the derivatives of R(z) are non-zero at the start of the contraction, and so no term beyond the leading order in the above naive expansion satisfies the inlet conditions.

For the hyperbolic geometry (4), there is a considerable simplifica-

$$\frac{1}{R^2} \left(\frac{1}{R^2} \right)' = \frac{\beta}{R^2}.$$

Hence

$$b_{22} = \frac{1}{R^2} \left(1 - De\beta F + De^2\beta^2 F^2 - De^3\beta^3 F^3 + \cdots \right).$$

Summing

$$b_{22}^{sim} = \frac{1}{R^2} \frac{1}{1 + De \beta F}.$$
 (13)

This is exactly the similarity solution of Sialmas & Housiadas [1], see their Eq. (45). In the above, De is the entrance Deborah number and $De\beta = De_e$ is the Deborah number based on the axial strain-rate, see Eq. (16). Hence rewriting

$$b_{22}^{sim} = \frac{1}{R^2} \frac{1}{1 + De_o F},\tag{14}$$

Clearly b_{22}^{sim} fails to satisfy the inlet condition $b_{22} = 1$ at x = 0. The solutions for the other components of the deformation tensor are

$$b_{12}^{sim} = \frac{1}{R^2} \frac{1}{(1 + De_{\rho}F)^2}, \quad b_{11}^{sim} = \frac{1}{R^2} \frac{1}{(1 + De_{\rho}F)^3}.$$
 (15)

These components also fail to satisfy the inlet conditions. By $De_eF=1$, the similarity solution b_{11}^{sim} fails to satisfy the inlet condition by factor of 8. Note that the series expansions have a finite radius of convergence at $De_e=\frac{1}{2}$, due to a pole at $2De_e=1$. This pole is the standard infinite viscosity of Oldroyd-B at a finite strain-rate, seen in lubrication theory only in an expansion $(-1 < \beta < 0)$ and not in a contraction $(\beta > 0)$.

In their derivation of the similarity solution Sialmas & Housiadas [1] assume in the first sentence of their §4.2, with Eq. (20), a simple downstream dependence for the velocity and the components of stress, each multiplied by a self-similar dependence across the flow. In particular, they assume for the velocity

$$w(\rho,z) = \frac{F(\rho = r/R(z))}{R^2(z)}.$$

Thus each streamline, $\rho = \text{const.}$, is a scaled copy of the boundary of the contraction. For the hyperbolic contraction, $1/R^2 = 1 + \beta z$, all the streamlines are hyperbolae, and the axial strain rate for a streamline is

$$e = \frac{\partial w}{\partial z} = \beta F(\rho). \tag{16}$$

Thus the strain-rate is constant along each streamline, a different constant on different streamlines. The key to obtaining the simple similarity solution is that all the streamlines, possibly not Newtonian, are hyperbolae on which the axial strain-rate is constant. On each streamline, the cross-flow stress A_{22}^{sim} does not see the shear between the streamlines and responds as if it is in a uniform uni-axial extensional flow. Thus $A_{22}^{sim} = 1/(1 + De_e F)$, with axial strain-rate for that streamline De_eF . It is the bi-axial compression rather than the uni-axial stretching that is reducing the magnitude of the cross-flow component of stress. Note that this component of stress has the standard infinite viscosity at a finite (negative) strain-rate for Oldroyd-B in extensional flows. Starting from this component of stress, the shear-rate Def/R^3 between the streamlines produces the elastic shear component of stress, $A_{12}^{sim} =$ $Def/(R^3(1+De_{\rho}F)^2)$. Shearing this component produces the tension in the streamlines, $A_{11}^{sim} = 2De^2f^2/(R^6(1+De_eF)^3)$. Note all components decrease as 1/De at high De. This explains why the similarity solution produces vanishing elastic contribution to the pressure drop as De increases. While the internally generated elastic stresses of the similarity solution are decreasing, the stresses in the full solution become dominated by the shearing and stretching of the inlet elastic stresses.

Substituting the similarity solution (14) and (15) into expression (9) for the pressure drop, and then expanding in small De_e , we have the elastic contribution to the pressure drop

$$\Delta p_e^{sim} = 8(1+\beta+\frac{1}{3}\beta^2)\left(1-4De_e+10De_e^2-\frac{112}{5}De_e^3+48De_e^4\right). \tag{17}$$

This agrees with the $O(\eta)$ terms (first elastic effects) in equation (63) of Sialmas and Housiadas, noting their $De_m = \frac{1}{2}De_e$.

The similarity solution obtained by Sialmas & Housiadas [1] is more general than that found here, in that it applies to arbitrary concentration c for which the velocity no longer has the Newtonian parabolic. In the results (14) and (15), one need only replace $F(\rho)$ by the non-parabolic velocity profile and set $f(\rho) = F'(\rho)$ to be the associated shear profile. While the velocity profile does change from the Newtonian, there is a theorem of Tanner & Pipkin [6] which says that it remains unchanged at O(De) at low De. At high De, the elastic stresses in the similarity solution decrease as 1/De, except in a thin layer next to the boundary, so that the velocity becomes Newtonian again.

5. Full solution

While the naive expansion in small De fails to satisfy the inlet boundary conditions at all orders beyond the first, Fig. 2 shows that the full solution and similarity solutions agree well with the O(De) approximation. It also seems that the full solution and similarity solutions agree with one another very well to $De_e=0.9$. In this section we find an expression for the part that must be added to the similarity solution to make it the full solution.

To make further analytic progress, attention is restricted to a hyperbolic contraction (4). The similarity solution provides a so-called 'particular integral' to the Oldroyd-B Eqs. (6), forced by the term R^{-2}

in the bracket on the right hand side of Eq. ((6)a). We now need a so-called 'homogeneous solution' to Eqs. (6) with the R^{-2} term dropped. This homogeneous solution will enable the inlet stress conditions to be satisfied. Write the full solution as the similarity solution plus an extra part,

$$b_{ij} = b_{ij}^{sim} + b_{ij}^{+}. (18)$$

The inlet conditions on the extra part are

$$b_{ij}^{+}(0,\rho) = 1 - b_{ij}^{sim}(0,\rho).$$
 (19)

The solution for the extra part is found to be

$$b_{22}^{+} = (1+\zeta)^{-1/\alpha} b_{22}^{+}(0,\rho), \tag{20a}$$

$$b_{12}^{+} = (1+\zeta)^{-1/\alpha} \left(b_{12}^{+}(0,\rho) + \frac{b_{22}^{+}(0,\rho)}{\alpha} \ln(1+\zeta) \right), \tag{20b}$$

$$b_{11}^{+} = (1+\zeta)^{-1/\alpha} \left(b_{11}^{+}(0,\rho) + \frac{b_{12}^{+}(0,\rho)}{\alpha} \ln(1+\zeta) + \frac{b_{22}^{+}(0,\rho)}{2\alpha^{2}} \ln^{2}(1+\zeta) \right). \tag{20c}$$

where

$$\zeta = \beta z$$
 and $\alpha = De_{\rho}F$.

Sialmas & Housiadas [1] found in their Eq. (51) an expression for $\sigma_{yy}(y=0,z)$ similar to ((20a)) above.

By definition, small De means that the residence time is much longer than the relaxation time. Hence at low De all the extra parts have time to relax near to the inlet. Thus

$$(1+\zeta)^{-1/\alpha} = \exp\left(-\frac{1}{De\beta F}\ln(1+\beta z)\right) \sim \exp\left(-\frac{1}{DeF}z\right) = e^{-z/DeF}. \tag{21}$$

The O(De) error in the naive expansion failing to satisfy the inlet conditions therefore decays in a short O(De) distance, and so makes a net $O(De^2)$ contribution to the pressure drop. Hence the good agreement of the O(De) approximation in Fig. 2. We now look to higher order corrections using solution (20).

There are two integrals along streamlines in expression (9) for the pressure drop. For the normal stress term

$$\begin{split} &\int_{0}^{1} \frac{1}{R^{2}} \frac{\partial}{\partial z} \left(\frac{b_{11}^{+}}{R^{2}} \right) dz, \\ &= -b_{11}^{+}(0) - \int_{0}^{\beta} (1+\zeta)b_{11}^{+} d\zeta, \\ &= -b_{11}^{+}(0) - \int_{0}^{\beta} (1+\zeta)^{-(1/\alpha-1)} \left(b_{11}^{+}(0) + \frac{b_{12}^{+}(0)}{\alpha} \ln(1+\zeta) + \frac{b_{22}^{+}}{2\alpha^{2}} \ln^{2}(1+\zeta) \right) d\zeta, \\ &= -b_{11}^{+}(0) - \frac{\alpha b_{11}^{+}(0)}{1-2\alpha} - \frac{\alpha b_{12}^{+}(0)}{(1-2\alpha)^{2}} - \frac{\alpha b_{22}^{+}(0)}{(1-2\alpha)^{3}}. \end{split}$$

Here it has been assumed that the integrals are dominated by contributions from near the inlet, while the contributions from near the outlet, which are $O((1+\beta)^{1/\alpha-2})$, are exponentially small. This requires $De_eF<\frac{1}{2}$ for all F, i.e. $De_e<\frac{1}{4}$. For the elastic shear stress term

$$\int_{0}^{1} \frac{b_{12}}{R^{2}} dz,$$

$$= \frac{1}{\beta} \int_{0}^{\beta} (1+\zeta)^{-(1/\alpha-1)} \left(b_{12}^{+}(0) + \frac{b_{22}^{+}(0)}{\alpha} \ln(1+\zeta) \right) d\zeta,$$

$$= \frac{1}{\beta} \left(\frac{\alpha b_{12}^{+}(0)}{1-2\alpha} + \frac{\alpha b_{22}^{+}(0)}{(1-2\alpha)^{2}} \right),$$
(23)

again including only contributions from near the inlet.

The inlet conditions (19) on the b_{ij}^+ are found from the similarity solution (14) and (15) evaluated at the inlet where R=1. Expanding in small $\alpha=De_eF$

$$b_{22}^+(0,\rho) = \alpha - \alpha^2 + \alpha^3 + \cdots,$$

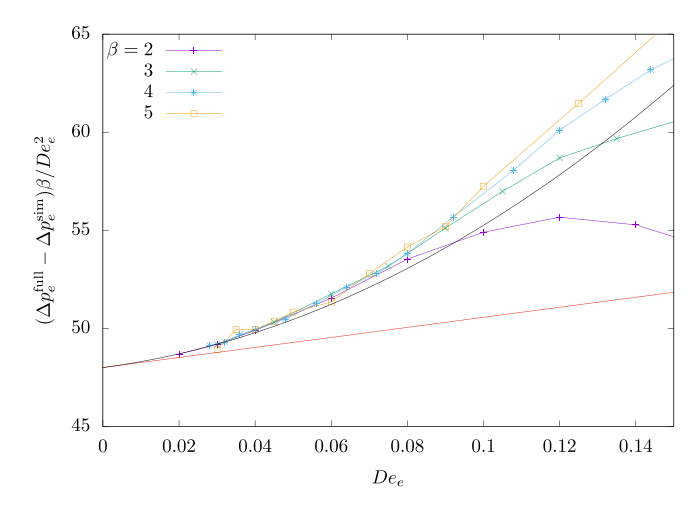


Fig. 3. The difference between the numerical results for the pressure drop as predicted by the full solution and that predicted by the similarity solution, for $\beta=2$, 3, 4 and 5. Plotted is the difference divided by De_e^2/β as a function of De_e . The red line is the linear approximation $48+25.6De_e$. The black curve is the quadratic approximation $48+25.6De_e+469.333De_e^2$.

$$b_{22}^{+}(0, \rho) = 2\alpha - 3\alpha^{2} + 4\alpha^{3} + \cdots,$$

$$b_{22}^{+}(0, \rho) = 3\alpha - 6\alpha^{2} + 10\alpha^{3} + \cdots.$$

Substituting these into (22) and (23) and expanding further in small α

$$\int_0^1 \frac{1}{R^2} \frac{\partial}{\partial z} \left(\frac{b_{11}^+}{R^2} \right) dz = -3\alpha - 20\alpha^3 + \cdots,$$

$$\int_0^1 \frac{b_{12}}{R^2} dz = \frac{1}{\beta} \left(3\alpha^2 + 4\alpha^3 + 15\alpha^4 + \cdots \right).$$

Combining these in the expression (9) for the elastic contribution to the pressure drop and integrating across the streamlines, we have at small De

$$\Delta p_e^+ = \frac{1}{6} \left(48 D e_e^2 + \frac{128}{5} D e_e^3 + \frac{1408}{3} D e_e^4 + \dots \right). \tag{24}$$

This shows that the pressure drop of the similarity solution deviates from that of the full solution at $O(De^2)$.

Prediction (24) is tested in Fig. 3 in which the difference between numerical results for the pressure drop of the similarity are subtracted from the numerical results for the full solution. These numerical results were given earlier in Fig. 2. The deviation of the pressure drops is divided by De_e^2/β and plotted as a function of De_e . Also plotted are the linear and quadratic predictions of (24). All the results are within the restriction of $De_e < 0.25$ for the inlet contribution to be larger than the exit contribution in the various integrals. The results come together in the range $0 < De_e < 0.1$, and seem to be approaching the quadratic approximation in $De_e < 0.05$.

It can be seem that the results for the contraction ratio of $\beta=5$ are a little wobbly. The problem is that at $De_e=0.03$ and $\beta=5$ the relative difference between the two solutions is less that 10^{-4} , which is pushing the here 6-figure accuracy of the numerical results. The loss of accuracy becomes more acute at $\beta=15$. This is why this test has been performed at more modest contraction ratios, demonstrating universality of the asymptotic prediction.

While the expansions for the pressure drop differ at $O(De^2)$, the curves in Fig. 2 remain remarkably close to $De_e=0.75$ for $\beta=15$. This can be explained by the magnitude of the coefficients of the $O(De_e^2)$ terms, 7283.2 for the full solution and 7280 for the similarity solution for $\beta=15$. Comparing expressions (17) and (24), one sees that at each order De_e^n the coefficients in two pressure drops are greater than their difference by a factor of β^3 , which is over 3000 for $\beta=15$. Most of the pressure drop comes from near the exit where $R^{-4}=O(\beta^2)$,

see Eq. (8). At low De most of the difference between the full and similarity solutions comes from near the entrance, see Eq. (21). This gives the factor of β^3 between the coefficients of the expansions and their difference.

The relatively small difference between the coefficients explains the remarkable agreement between the full and similarity solutions in Fig. 2 at $De_e \lesssim 1$. The divergence between the two solutions at higher De_e must therefore depend on terms beyond all orders in the expansions in De_a^n .

At low De the similarity solution nearly satisfies the inlet boundary condition, missing by O(De). By $De\beta=0.5$, the similarity solution accommodates less than half the inlet elastic shear stress and one third of the inlet normal stress. The calculation of the pressure drop coming from the extra parts of the inlet stresses, above those in the similarity solution, involves an integral along each streamline of the form

$$\beta \int_0^1 (1+\beta z)^{(1-1/De\beta F(\rho))} dz = \frac{1}{(1/De\beta F - 1)} \left(1 - (1+\beta)^{(2-1/De\beta F)} \right), (25)$$

and two similar integrals with additional logarithmic factors, see (22) and (23). At low-De, the integrand is asymptotically $e^{-z/DeF}$, see Eq. (21), so the integral is $De\beta F$ (first terms dominating in the two brackets on the right hand side). The additional inlet stresses decay exponentially near the entrance to the contraction while $De\beta F < \frac{1}{2}$. All changes at $De\beta F = \frac{1}{2}$, when the whole range of integration starts to contribute. While the extra inlet stresses are still relaxing, more slowly because they are travelling faster at the higher De, the inlet stresses are also being stretched and so increasing.

The switch from good to poor agreement of predictions of the pressure drop between the similarity and full solutions is now explained by this change in the where the contributions to the integral come from, the change occurring at $De\beta F=\frac{1}{2}$. Now $F(\rho)$ varies across the streamlines, taking values between 0 and 2. The different streamlines contribute to the pressure gradient with a weighting something like $\rho^3(1-\rho^2)$, with the maximum contribution at $\rho^2=0.6$, where F=0.8. This suggests that the switch between good and poor agreement should occur around $De\beta=\frac{5}{8}$, which is confirmed by Fig. 2 above.

6. Conclusion

The main conclusion of this paper is that the full solution that satisfies the inlet stress boundary condition approaches the similarity solution if the residence time is longer than the relaxation time. This is measured by a Deborah number based on the strain-rate being small, $De_e \lesssim 1$. Thus predictions of the pressure drop by the similarity solution agree with the full solution for small De_e , remarkably well for the areacontraction ratio studied, $1 + \beta = 16$. For larger $De_e \gtrsim 1$, the similarity solution predicts that the elastic contribution to the pressure drop tends to zero, while the full solution decreases linearly with De_e . The similarity solution tends to zero is because all the stresses are tending to zero, are O(1/De). The full solution decreases linearly because the tension in the streamlines pulls the flow through the contraction which therefore needs less pressure to push it, see [2]. Figure 5 of Sialmas & Housiadas [1] shows their prediction by the similarity solution of the total pressure drop tending at their $De_m = 1$ ($De_e = 2$) to $1 - \eta$, their solvent viscosity value, i.e. the elastic polymer contribution tending to zero.

There must be a concern that the decreasing pressure drop with increasing flow might lead to a mechanical instability. This would be true for a Newtonian viscous fluid. For a viscoelastic fluid, it is not the pressure drop which determines the stability, but the difference in the total forces exerted across the inlet and exit. The total forces include contributions from the tension in the streamlines, as explained above the very cause of the reduction in the pressure drop. One must also note that the pressure drop calculated here is just the pressure drop in the contraction. The outflow of the contraction must be attached to something, and that will introduce further adjustments in the pressure.

If the outflow is attached to a wide bath or to an expansion to a pipe with a diameter equal to the inlet diameter, then the effect of the tension in the streamlines is entirely cancelled.

The slowly varying contraction is an interesting rheological flow, a mix of high shear and moderate axial extension. In the special case of a hyperbolic contraction, there is a similarity solution, and it has streamlines that are all hyperbolae, along which the extension-rate is constant. The cross-flow component of stress σ_{22} only reacts to the squeezing together of the streamlines by the extensional part of the flow. The other components are generated by the strong shear of this cross-flow component.

In Section 4, an expansion was made in small De. The naive expansion offered no opportunity to satisfy any inlet boundary conditions. In order to satisfy the inlet condition, axial derivatives of the shape had to vanish at the entrance, and they do not vanish for the hyperbolic shape. The terms of the expansion can be summed, the sum being precisely the similarity solution, and it does not satisfy the inlet condition. Clearly there must be a good agreement between the expansion and the similarity solution, the latter being the sum of the former, but that good agreement offers no support that either are correct. There are a number of recent articles, amongst them [7–9], which exhibit low-De expansions with multiple derivatives of the shape of the boundary, derivatives which do not exist at the entrance for hyperbolic shape being used.

While there is remarkably good agreement in $De_e < 1$ between the predictions for the pressure drop given by the full and the similarity solutions, the predictions diverge at $De_e = 1$. The divergence was found at the end of Section 5 to be due to a switch from where the dominant contributions to integral (25) come. At low-De, the dominant contributions come from near the entrance, with the exit contributions exponentially small (beyond all orders in De^n). At $De_eF(\rho) = 0.5$, the dominant contributions switch to being from near the exit. This is reminiscent of the behaviour in exponential asymptotics. For example consider figure 3.3 on page 36 of [10] for the integration contour for the Airy function Ai(z). As arg(z) passes from less than π to greater than π , the dominant saddle point switches.

CRediT authorship contribution statement

John Hinch: Conceptualization, Data curation, Formal analysis, Investigation, Methodology, Software, Validation, Writing – original draft, Writing – review & editing.

Declaration of competing interest

The authors declare that they have no known competing financial interests or personal relationships that could have appeared to influence the work reported in this paper.

Data availability

Data will be made available on request.

References

- Panagiotis Sialmas, Kostas D. Housiadas, An exact solution of the lubrication equations for the Oldroyd-B model in a hyperbolic pipe, J. Non-Newton. Fluid Mech. 335 (2025) 105331
- 2] John Hinch, Evgeniy Boyko, Howard Stone, Fast flow of an Oldroyd-B model fluid through a narrow slowly varying contraction, J. Fluid Mech. 988 (2024) A11.
- [3] David F. James, Caitlin A.M. Roos, Pressure drop of a Boger fluid in a converging channel, J. Non-Newton. Fluid Mech. 293 (2021) 104557.
- [4] Evgeniy Boyko, John Hinch, Howard A. Stone, Flow of an Oldroyd-B fluid in a slowly varying contraction: theoretical results for arbitrary values of Deborah number in the ultra-dilute limit, J. Fluid Mech. 988 (A10) (2024).

- [5] M. Renardy, How to integrate the upper convected Maxwell (UCM) stresses near a singularity (and may be elsewhere), J. Non-Newton. Fluid Mech. 52 (1994) 91–95
- [6] R.I. Tanner, A.C. Pipkin, Intrinsic errors in pressure-hole measurements, Trans. Soc. Rheol. 13 (1969) 471–484.
- [7] Evgeniy Boyko, Howard A. Stone, Pressure-driven flow of the viscoelastic Oldroyd-B fluid in narrow non-uniform geometries: analytical results and comparison with simulations, J. Fluid Mech. 936 (2022) A23.
- [8] Kostas D. Housiadas, Antony N. Beris, Pressure-driven viscoelastic flow in axisymmetric geometries with application to the hyperbolic pipe, J. Fluid Mech. 999 (2024) A7.
- [9] Bimalendu Mahapatra, Tachin Ruangkriengsin, Howard A. Stone, Evgeniy Boyko, Viscoelastic fluid flow in a slowly varying planar contraction: the role of finite extensibility on the pressure drop, J. Fluid Mech. 1009 (2025) A12.
- [10] E.J. Hinch, Perturbation Methods, Cambridge University Press, 1991.